buildings

MDPI

Article

Seismic Hazard Curve as Dynamic Parameters in Earthquake Building Design for Sabah, Malaysia

Noor Sheena Herayani Harith [1,2,*], Felix Tongkul [2] and Azlan Adnan [3]

[1] Faculty of Engineering, Universiti Malaysia Sabah, Jalan UMS, Kota Kinabalu 88400, Sabah, Malaysia
[2] Natural Disaster Research Centre (NDRC), Universiti Malaysia Sabah, Jalan UMS, Kota Kinabalu 88400, Sabah, Malaysia
[3] School of Civil Engineering, Universiti Teknologi Malaysia, Johor Bahru 81310, Johor, Malaysia
* Correspondence: sheena@ums.edu.my

Abstract: This paper presents the significance of a seismic hazard curve plot as a dynamic parameter in estimating earthquake-resistant structures. Various cases of structural damages in Malaysia are due to underestimating earthquake loadings since mostly buildings were designed without seismic loads. Sabah is classified as having low to moderate seismic activity due to a few active fault lines. Background point, area, and line sources are the three tectonic features that have impacted Sabah. Data on earthquakes from 1900 to 2021 have been collected by a number of earthquake data centers. The seismicity is based on a list of historical seismicities in the area, which stretches from latitudes 4 °S to 8 °N and longitudes 115 °E to 120 °E. The goal of this research is to develop a seismic hazard curve based on a conventional probabilistic seismic hazard analysis being examined for the maximum peak ground acceleration at 10% probability of exceedance as published in MSEN1998-1:2015. This study extended to 5% and 2% probability of exceedance combined with the seismic hazard curve by using Ranau as a case study. To calculate the expected ground motion recurrence, such as peak ground acceleration at the site, earthquake recurrence models were combined with selected ground motion models. A logic tree structure was used to combine simple quantities such as maximum magnitudes and the chosen ground motion models to describe epistemic uncertainty. The result demonstrates that peak ground acceleration values at the bedrock were estimated to be 0.16, 0.21, and 0.28 g of the total seismic hazard curve at 10%, 5%, and 2% PE in a 50-year return period, respectively. The seismic hazard study at a Ranau site basically depends on the seismicity of a region and the consequences of failure in the past. Thus, the results can be used as a basis for benchmarking design or evaluation decisions and for designing remedial measures for Sabah constructions to minimize structural failure.

Keywords: hazard curve; moderate earthquake; design standard; structural failure

Citation: Harith, N.S.H.; Tongkul, F.; Adnan, A. Seismic Hazard Curve as Dynamic Parameters in Earthquake Building Design for Sabah, Malaysia. *Buildings* **2023**, *13*, 318. https://doi.org/10.3390/buildings13020318

Academic Editors: Rafael Shehu, Nicola Tarque and Manuel Buitrago

Received: 6 December 2022
Revised: 11 January 2023
Accepted: 16 January 2023
Published: 20 January 2023

1. Introduction

Earthquakes are a sequence of movements caused by a sudden release of energy due to fault displacement. This seismic vibration can cause the earth to shake, potentially affecting heavily populated areas and resulting in human injury and death. Thus, buildings and nonstructural elements must be able to withstand seismic loads to reduce the number of deaths from these incidents. Alberto et al. [1] found that securing building safety is essential based on their examination of building failure. Furthermore, as demonstrated by Perrone et al. [2], nonstructural elements must also improve seismic regulations because this type of structure performs poorly during earthquakes. Malaysia is located on the stable Eurasian plate to the south and within stable continental regions (SCR). Large earthquakes are considered to occur relatively infrequently in SCR, and if they do, there also will inevitably be damage. In SCR, faults are often unknown, and seismic source characteristics are subject to greater uncertainty. The deformation of Southeast Asia was a combined result

of continental collision and oceanic subduction [3]. However, Malaysia is very fortunate despite being surrounding by countries with large earthquakes, but its position is stable in the Eurasian Plate. Malaysia's location is also geographically outside of the ring of fire [4].

A significant or even moderate shallow-focus earthquake is usually accompanied by several other tremors. The biggest challenge is the PGA value that should be taken that corresponds to the moderate area. The representation of uniform seismicity characteristics, such as focal depth, seismicity intensity, and maximum magnitude, are represented by seismic source zones. Geological, seismological, geophysical, and geotechnical investigations are used to create the characterizations. Each piece of earthquake data is selected from within an enclosed region that is likely to occur within a source zone of seismicity and tectonism that is similarly associated. Because of the high rate of occurrence of events and the vast amount of research conducted in those active tectonic areas, the localization of faults that trigger earthquakes is also very accurate but not a moderate region. The limited amount of earthquake data, on the other hand, is not a factor in predicting potential earthquakes in seismic hazard analysis. Borah et al. [5] found that source zonation is a significant factor in hazard estimation. Sawires and Hamdache [6] agreed on the importance of characterizing the earthquake source using logic tree approach, especially in low-rate seismicity regions, in order to improve seismic hazard assessment.

The method of quantitatively assessing the design parameters of earthquake ground motion at a specific site is known as probabilistic seismic hazard analysis, or PSHA. Peak ground acceleration (PGA) is a ground motion metrics that are taken into account in this evaluation. There are four procedures that PSHA should follow: (1) gathering earthquake data, (2) describing the seismic source's size and distance, (3) identifying the earthquake's ground motion, and (4) computing the seismic hazard at certain sites. In the current investigation, the PGA value at 10% PE is benchmarked based on MSEN1998-1:2015 [7] as similarly conducted by Drouet et al. [8]. MSEN1998-1 [7], Malaysia's first national seismic hazard maps, were completed in 2017 and are based on Eurocode 8 [9]. This broad view of earthquakes is used to assess the current earthquake situation throughout Malaysia. The identification of active faults is an essential component in seismic hazard analysis. Faults might be either active or inactive. When referring to moderate seismicity, the term "active" denotes movement, even if it is of small magnitude. Therefore, in the zoning procedure where the seismic events are not populated, there may be numerous uncertainties. According to Sharon et al. [10], the seismic source zone identification in this instance was achieved by assuming a consistent rate of seismicity throughout each distinct source zone and using sufficient geological and paleoseismic data to specify source locations. Therefore, current geological maps of Sabah by Wannier [11] and Mohd Zainudin et al. [12] are used for the delineation of fault source identification.

In the preceding 121 years, Sabah has seen 520 earthquakes with magnitudes ranging from 2.9 to 6.3. According to Agarwal and Blockley [13], damage is required for failure to occur, and hazard is required for damage to occur. The seismic hazard study at a location is mostly determined by the region's seismicity, the sorts of structures involved, and the repercussions of failure, such as in the case of Ranau, Sabah. As a result, developing a Malaysian hazard curve is critical, particularly when it comes to seismic appraisal of existing buildings or new building development, particularly nonlinear response analysis. Using the existing earthquake database collection, the hazard curve suitable for Malaysia is examined using probabilistic seismic hazard assessment based on the highest recorded PGA value.

The possibility of exceeding a specific value in a predetermined future time period was referred to as the probability of exceeding it. For common buildings, 10% PE with a time period of 50 years is typically employed, as discovered in Looi et al. [14] and Chong et al. [15]. Three areas of research are being examined for their maximum PGA based on prior seismic activity predictions in the region, as published in MSEN1998-1:2015 [7]. According to Looi et al. [16], the highest PGAs for Sabah, Sarawak, and West Malaysia are 0.15, 0.11, and 0.11 g, respectively. Sabah has a PGA value of 0.16 g on the National Hazard

Map, MSEN1998-1:2015 [7], whereas Sarawak has a value of 0.15 g, and West Malaysia has a value of 0.13 g. Based on a global assessment utilizing the global earthquake model (GEM), Pagani et al. [17] estimated the PGA value at 10% PE to be between 0.08 and 0.13 g. As noted in the PGA comparison, Sabah has the highest PGA in comparison with Sarawak and West Malaysia (Table 1). This study accumulated the hazard curve of Sabah based on hazard value summarized from MSEN1998-1:2015 [7]. Seismic hazard curve is the size and frequency of seismic action to which a region may be subjected for a certain period of time. The curve reflects the seismic parameters, source characteristics, and types of earthquakes in the region.

Table 1. Expected maximum PGA values in Sabah, Sarawak, and West Malaysia assuming a 10% probability of exceedance.

Reference	PGA at 10% PE (g)		
	Sabah	**Sarawak**	**West Malaysia**
Looi et al. [16]	0.15	0.11	0.11
MSEN1998-1:2015 [7]	0.16	0.15	0.13
Pagani et al. [17]	0.13	0.13	0.08

In order to determine the effect of seismic loads on various types of structures, earthquake-resistant loadings of 10%, 2%, and 5% are investigated. The three types of PE are an extensive analysis for further analyzed buildings under various scenarios, as performed by Yang et al. [18], and Dutfoy [19] analyzed 10%, 5%, and 2% as new-generation probabilistic seismic hazard information as an alternative seismic hazard modelling. In the seismic design analysis of different types of structure, Tr 475 and 1000 years are known as operating basis earthquake (OBE) seismic level equivalent to 10% and 5% of PE, respectively, and Tr 2475 is safe shutdown earthquake (SSE) seismic level equivalent to 2% of PE. The seismic design of structures is generally based on a design response spectrum obtained from hazard analysis for a specified return period. For many engineering applications, such as the design of critical facilities or highly irregular buildings, a more complex dynamic nonlinear analysis is often conducted. Such analysis requires input in the form of design time series with response spectra that are consistent with the target design spectrum. Earthquake acceleration time histories (EATH) known also as design time series are developed by modifying initial time series that consist of empirical recordings from past earthquakes representative of the design event or numerical simulations of the ground motion for the design event. Two approaches exist for modifying the time series to be consistent with the design response spectrum: scaling and spectral matching. Scaling involves multiplying the initial time series by a constant factor so that the spectrum of the scaled time series is equal to or exceeds the design spectrum over a specified period range. Spectral matching involves modifying the frequency content of the time series to match the design spectrum at all spectral periods [20]. The synthetic earthquake acceleration time histories (EATH) on the rock site condition for all the interest return periods are proposed for dynamic structural analysis purposes. The earthquake acceleration time histories are provided based on a range of earthquake intensity measures by using several real recorded data and performing the spectral matching algorithm.

2. Methods

In common analysis of linear and nonlinear dynamic, response spectrum would refer to linear elastic analysis. The hazard curve is a plot that can be transformed into a response spectrum at different period procedures able to assess the seismic vulnerability in a probabilistic manner, such as in the investigations of Marmureanu et al. [21], Solarino and Giresini [22], and Vargas-Alzate et al. [23], in comparison with nonlinear inelastic, which depends on the time history input, which requires a certain spectral matching analysis in a more complex manner. Seismic hazard analysis determines the probability of experiencing

a certain severity of any damaging earthquake at a specific location within a given time period [24,25]. It is a probabilistic mathematical procedure that evaluates the answer to uncertainty about future seismic location, earthquake size, and shaking intensity. As seen in the flowchart of methodology in Figure 1, the technique is divided into six phases, and each step is explained in greater detail in the following section.

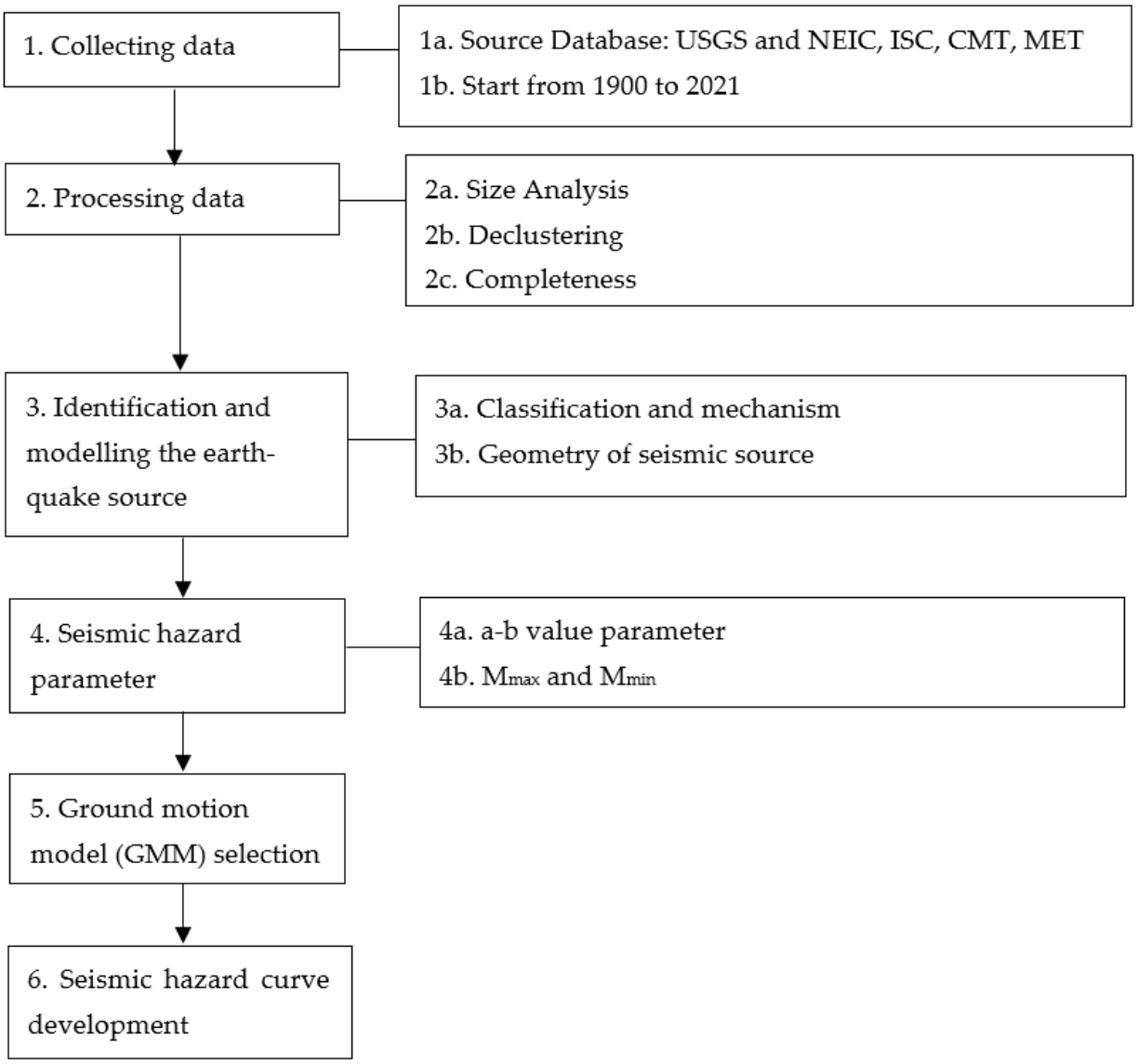

Figure 1. Process flow of the methodology of the work.

2.1. Data Collection and Processing Earthquake Catalog

The first step is to collect earthquake data. Various earthquake data centers have provided earthquake catalogue data spanning the years 1900 to 2021. The seismicity is based on a list of the region's historical seismicities, which spans latitudes 4 °S to 8 °N and longitudes 115 °E to 120 °E. Seismic occurrences with a magnitude greater than 2.0 are considered when compiling the catalogue. A massive dataset supported by numerous national and international agencies was used to compile earthquake databases, including the United States Geological Survey and National Earthquake Information Center (USGS and NEIC), International Seismological Centre (ISC), Harvard Centroid Moment Tensor (CMT), and Malaysian Meteorological Department (MET Malaysia). Following the collection of earthquake events, the next step is to analyze the magnitude of earthquakes, with the whole set in the earthquake catalogue being classified in terms of M_W. The most

accurate magnitude to classify the scale of an earthquake in seismic hazard analysis and moment magnitude is M_W since it is directly proportional to the algorithm of seismic moment and has a uniform behavior for all magnitude ranges. Since the accuracy of recorded earthquakes is dependent on magnitude, seismic hazard assessment needs a homogenous earthquake catalogue for the region studied [26–29].

The declustering procedure is then initiated. Several events in a cluster that occurred in conjunction with a main shock may have been dependent events (fore- and aftershocks) throughout the declustering process. These fore- and aftershocks must be removed from the collection using a declustering technique to ensure a distribution of earthquake occurrences. This study employs gridded seismicity zone analysis, as performed by Leptokaropoulos et al. [30] and Zaliapin and Ben-Zion [31], and density-based clustering from Cesca [32]. There were 172 events in the collection, declustered from 520 occurrences, with 5 events of M_W 6.0, 28 events of M_W 5.0, and 138 events of less than M_W 4.0. Declustering eliminates around 67% of the activities in the catalogue. This study investigates the completeness of earthquake data from 1900 to 2021. According to the data, earthquakes with magnitudes of less than M_W 4.0 were first completely documented beginning in 1980. All events with a magnitude greater than and equal to M_W 4.0 are fully reported in the 30-year earthquake database. This is because seismic stations have been installed in Malaysia since the late 1980s.

2.2. Identification and Modelling the Earthquake Source

The third stage is locating an earthquake source that is either active or inactive. The detection and delineation of seismic source zones is one of the main phases of a seismic hazard analysis. The features of the fault will include characteristics, such as focal depth, rate, and maximum magnitude. The tectonic features that affected Sabah can be categorized into three groups, as observed by Wannier [11] and Mohd Zainudin et al. [12], namely, point, area, and line sources, as sketched in Figure 2. A point source is a single, independent earthquake source, an area source is a fault that is dispersed over a wide area, and a line source is a fault that can be plainly visible on a map and has a specific length. This study performed a probabilistic seismic hazard assessment (PSHA) using the OpenQuake software developed by the Global Earthquake Model (GEM) [33].

2.3. Ground Motion Model Description

Ground motion parameters (peak ground acceleration, PGA) values can be calculated using an adequate set of ground motion models (GMMs), also known as ground motion prediction equation (GMPE), depending on the magnitude, source to site, and soil conditions of the earthquake source. According to multiple papers, including Anbazhagan et al. [34] and Weatherill and Cotton [35], using more than one GMM in logic tree formulations for PSHA has become normal practice. Thus, Table 2 lists three well-known GMMs used in the current study: Abrahamson and Silva [36], Zhao et al. [37], and Fukushima and Tanaka [38]. The PGA in this study was measured using Equation (1), which Abrahamson and Silva [36] constructed based on the next-generation attenuation (NGA) ground motion parameters:

$$\begin{gathered} \text{Ln Sa(g)} = f_1(M,R_{rup}) + a_{12}F_{RV} + a_{13}F_N + a_{15}F_{AS} + f_5(PGA_{1100},V_{S30}) + \\ F_{HW}f_4(R_{jb},R_{rup},R_x,W,dip,Z_{top},M) + F_{RV}f_6(Z_{top}) + (1 - F_{RV})f_7(Z_{top}) + f_8(R_{rup}) + \\ f_{10}(Z_{1.0},V_{S30}), \end{gathered} \tag{1}$$

where M stands for moment magnitude, R_{rup} is rupture distance (km), R_{jb} is Joyner-Boore distance (km), R_x is horizontal distance (km) from the top edge of the rupture, Z_{top} is depth to the top of the rupture (km), F_{RV} is flag for reverse faulting earthquakes, F_N is flag for normal faulting earthquakes, F_{AS} is flag for aftershocks, F_{HW} is flag for hanging wall sites, dip is fault dip in degrees, V_{S30} is shear-wave velocity over the top 30 m (m/s), $Z_{1.0}$ is depth to VS is 1.0 km/s at the site (m), PGA_{1100} is median peak acceleration (g) for V_{S30} = 1100 m/s, W is down-dip rupture width (km), and a_{12} to a_{15} are coefficients.

The shallow crustal earthquakes due to local faults were studied using the peak ground acceleration (PGA) ground motion parameters, the GMMs created by Zhao et al. [37] for shallow crustal earthquakes in Japan. Equation (2) describes the model:

$$\mathrm{Log}(y) = aM_W + bx - \log(r) + e(h-h_c)\delta_h + F_R + C_k + \varepsilon + \acute{\eta}, \quad (2)$$

where M_W denotes moment magnitude, x denotes source distance in kilometers, h denotes focal depth, δ_h is a dummy vector, F_R denotes reverse-fault parameter, C_k denotes site class, and ε and $\acute{\eta}$ denote coefficients. The equation was calibrated from rock, heavy, medium, and soft soil ground on the basis of earthquake data in Japan and other countries by Fukushima and Tanaka [38]. Although the model was created for Japan, it can be used in other countries with a distance of up to 300 km for M_W 4.6–8.2. Provided that M_W = moment magnitude and R = distance (km), the equation is shown in Equation (3).

$$\mathrm{Log}\ (\mathrm{PGA}) = 0.42M_W - \log(R+0.25 \times 10^{0.42M_W}) - 0.0033R + 1.22 \quad (3)$$

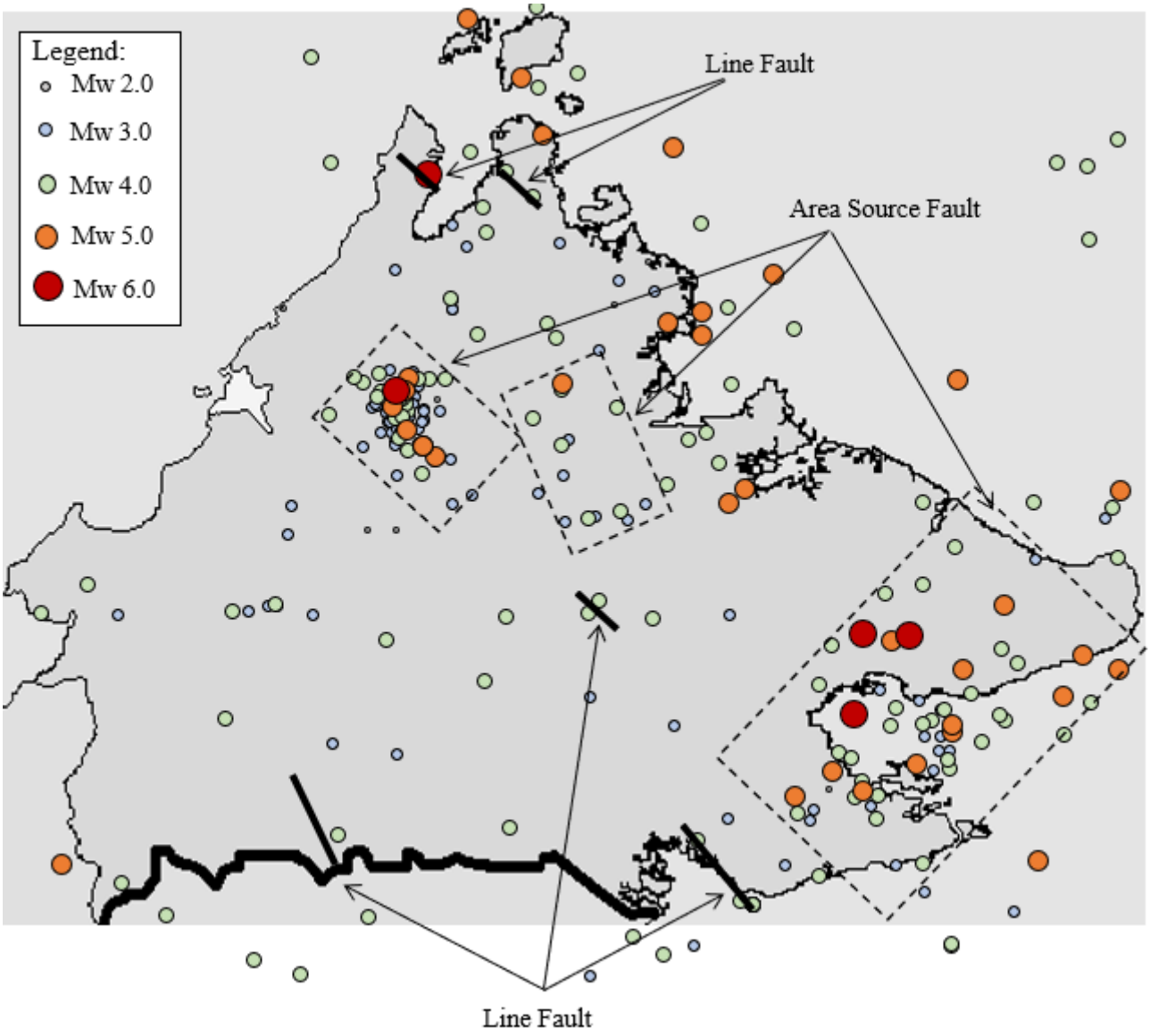

Figure 2. Plotted local seismicity and fault line framework of Sabah.

Table 2. Descriptions of the GMM used by PSHA to estimate the PGA ground motion parameters.

GMM Model	Description	Range of Magnitude	Distance Definition
Abrahamson and Silva [36]	Using the PEER NGA database, empirical ground motion models for the rotation-independent average horizontal component from shallow crustal earthquakes are created. The active shallow crust tectonic zone is supported.	5.0–8.5	Required distance measures at 0–200 km.
Zhao et al. [37]	Regression of historical data, primarily from Japan's subduction and crustal earthquakes, with data from earthquakes in the Western United States and the 1978 Tabas earthquake in Iran thrown in for good measure.	5.1–7.3	If a fault model is provided, the hypocentral distance (R_{hyp}), 0–300 km, is the shortest distance to the rupture plane (R_{rup}).
Fukushima and Tanaka [38]	Designed for active shallow crustal earthquakes.	4.6–8.2	Closest distance to the fault, 1–300 km.

The average shear wave velocity of 30 m depth, or V_{S30}, was employed. The classification of soil types is based on Eurocode 8, where 800 m/s is assigned to soil type A. There were a total of 367 earthquake time histories, comprising local earthquake events throughout Malaysia. These data originate from 70 earthquakes recorded by 33 seismic stations. Figure 3 depicts the magnitude, M_W and distance, R_{hypo} (km) distributions of records. It demonstrates that the majority of data are less than M_W 6.0 magnitude at a range of 5 to 600 km and greater than M_W 7.0 magnitude at distances greater than 500 km.

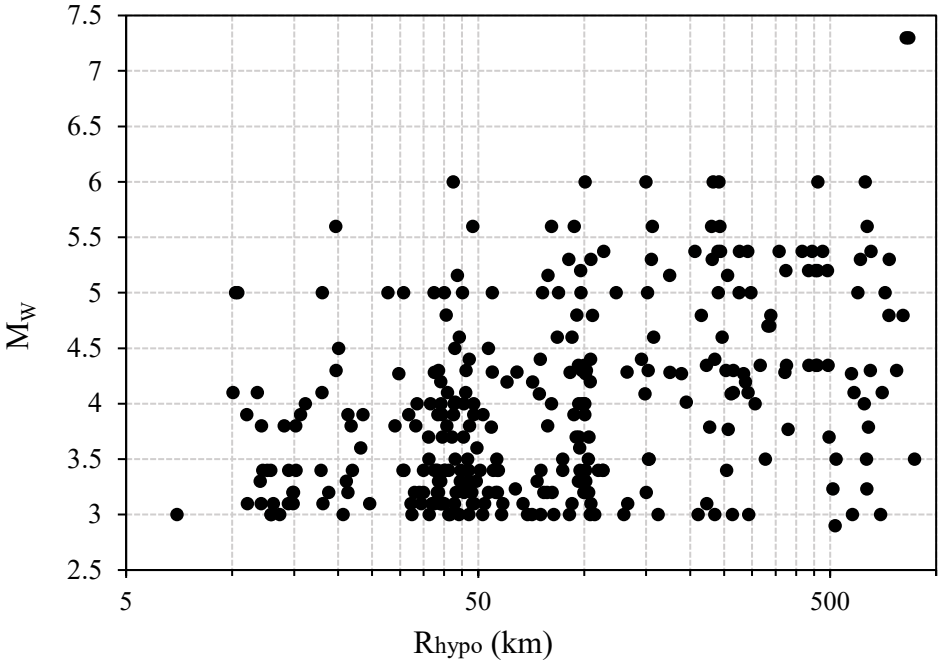

Figure 3. Distribution of data used in terms of magnitude and distance on EC8 soil class A.

In order to satisfy Sabah as being predominantly influenced by local seismic sources, the three selected GMMs were compared with real records on soil type A, as shown in Figure 4. The root of mean square (RMS) was determined for each model to measure

the difference between estimated and recorded PGA, following Tze et al. [39]. The error is defined as the difference between the estimated and recorded logarithmic values of PGA. The RMS value for the Fukushima and Tanaka [38] model is 0.869, followed by the Abrahamson and Silva [36] model at 0.415 and Zhao et al. [37] equal to 0.301.

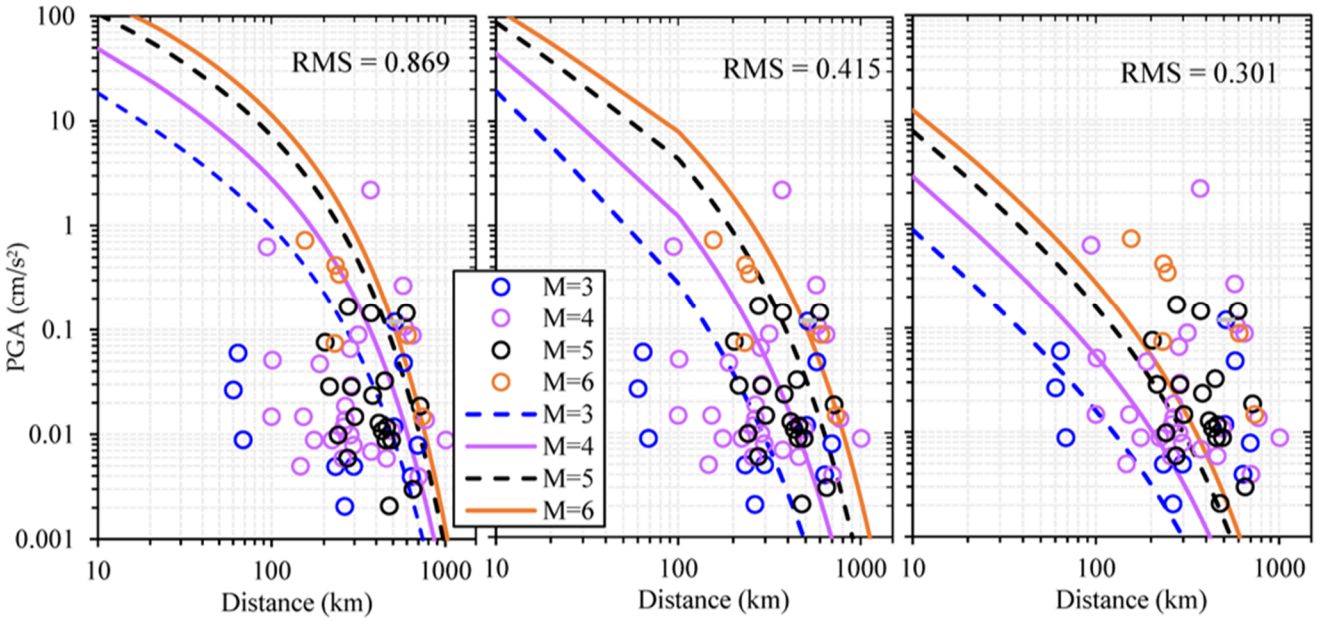

Figure 4. Comparison of GMM curves for active tectonic regions with recorded PGA on rock sites in Malaysia from local source earthquakes [36–38].

A logic-tree-based algorithm has recently been used to account for various types of uncertainties, such as the considered earthquake modelling, parameters of seismic source, maximum magnitude, and GMMs, which are analyzed for PSHA [28,34]. Multiple models were considered using logic trees, with weights that expressed the degree of confidence in the seismic hazard [35]. The technique is widely used as a tool to capture epistemic uncertainty in hazard estimation [6,28,34]. The probabilistic weights for the considered maximum magnitudes, as well as those for the earthquake source models for local faults that were chosen, were set based on the probability of each model's precision. According to Cummins [40] and Weatherill and Cotton [35], using proper GMMs has a bigger influence on PSHA; thus, to prevent conservative values from being over- and underestimated, the weight of each GMM is assigned to a logic tree. These three GMMs have good predictive and fitting capabilities for the observational data. The Abrahamson and Silva [36] model is shown to fit all magnitude ranges and distances between 10 and 1000 km the best. According to the hierarchy of curve-fitting GMMs, Zhao et al. [37] appears to be slightly underpredicted, whereas Fukushima and Tanaka [38] exhibits reasonable consistency, although a little overpredicted. The model of Abrahamson and Silva [36] demonstrated a perfect fit. The Abrahamson and Silva [36] equation was given the greatest weight of 0.5 since it offered better residual fits to the earthquake datasets. Fukushima and Tanaka [38] came in third with a weightage of 0.2, and Zhao et al. [37] obtained the second-highest weightage of 0.3. One form, weighted 1.0 in the all-source models, is used to compute the recurrence rate. The maximum magnitude is weighted by adding 0.5 to M_{max} and 0.25 to both $M_{max,+0.25}$ and $M_{max,-0.25}$.

2.4. Seismic Hazard Parameter

The basic input for the seismic hazard analysis is the source model, expressed through the Gutenberg–Richter recurrence for each of the seismic zones. The temporal distribution of earthquakes is assumed to follow a frequency–magnitude relationship. The Gutenberg–Richter recurrence model was used to calculate the seismic hazard parameters a, b, and

λ. In seismic hazard evaluations, the Gutenberg–Richter model is well known and widely accepted [19,41]. The maximum and minimum magnitude (M_{max} and M_{min}) can be determined using the previously compiled earthquake catalogue. The following formula can be used to calculate a, b, and λ: Log10 λ = a – bM, where λ is the earthquake rate and the a- and b-values are constant. The a-value represents the frequency of occurrence of events of a specific magnitude, whereas the b-value represents the relative distribution of small and large occurrence with β = 2.303 b. Table 3 summarizes the input of seismic hazard parameters for each source used to calculate the seismic hazard curve.

Table 3. Local faults' seismic hazard parameters.

Segment	Locality	Frequency–Magnitude Relationship		M_{max}
		β	λ	
Area	Lahad Datu	0.921	0.201	6.5
	Ranau		0.152	
	Labuk	0.824	0.043	5.5
Line	Kudat	0.921	0.152	6.0
	Pitas	0.824	0.043	5.0
	Perancangan			
	Pensiangan			
	Tawau			
	Kunak	1.051	0.175	6.0
Background	BS1	0.824	0.043	4.0
	BS2	1.051	0.175	5.5
	BS3			6.0

2.5. Seismic Hazard Curve Calculation

Until calculating the hazard curve, the next step was to use a probabilistic method to quantify design parameters of earthquake ground motion, such as peak ground accelerations at the bedrock. Baker et al. [42] established a complete probability theorem that will be used to measure the PSHA equation. This theorem is based on a probability principle, which treats the earthquake magnitude M and hypocenter distance R_{hyp} as continuous independent random variables. In its most basic form, the complete probability theorem is expressed by Equation (4).

$$P[I \geq i] = \int_R \int_M P[I \geq i | m \text{ and } r].f_M(m).f_R(r)dmdr \quad (4)$$

The equation consists of $f_M(m)$, where it is the magnitude density function, and $f_R(r)$ is the hypocenter distance density function. For a given earthquake magnitude M and hypocenter distance R, [I > i | m and r] is a conditional probability of (random) intensity I exceeding the value of i at the site. The natural logarithm of a number is logarithm to the base e, while the usual logarithm of a product is the sum of the logarithms of the numbers being multiplied. Equation (5) can be used to translate the relationship between the two logarithms.

$$Log_{10}(PGA) = \frac{\ln(PGA)}{\ln(10)} \quad (5)$$

The probabilistic seismic hazard analysis is computed to account for various return periods of the hazard for Sabah since it is dependent on the annual rate of ground motion exceeding a specific value. The likelihood of reaching the ground motion level z due to

an occurrence of size magnitude and distance length reflects a strong ground motion at a site due to all earthquakes predicted to occur in the area around the site. There is a probability of exceeding z during an exposure period of Y years, assuming that z is the average occurrence rate. The probability of exceeding Z during an exposure period of Y years can be written as in Equation (6).

$$P(Z > z) = 1 - \exp[-Yz] \quad (6)$$

The probability density function for magnitude, M, is based on the Gutenberg–Richter equation, which assumes that the upper bound of earthquake magnitudes is limited due to the finite size of the source faults. A bounded Gutenberg–Richter recurrence law is a finite magnitude distribution in which if a maximum magnitude is calculated, the likelihood of magnitude is expressed in Equation (7).

$$F_M(m) = \frac{bln(10).10^{-b(m-m_{min})}}{1 - 10^{-b(m_{max}-m_{min})}} \quad (7)$$

When it comes to earthquake sources, the likelihood of seeing a distance less than R is proportional to the fraction of the fault that is within a total length of r. In Equation (8), it is presumed that earthquake epicenters are equally probable in all places.

$$F_R(r) = P(R < r) \quad (8)$$

Additionally, probabilistic uniform hazard response spectra of the interested site can also be derived. A response spectrum in which each point has the same probability of exceedance during a specific design time is called uniform hazard spectrum (UHS) on a rock site (V_{S30} = 760 m/s). The calculated uniform hazard spectrum on a rock site is based on OBE and SSE seismic levels. The recommended elastic acceleration response spectra are based on part 1 of Eurocode 8 [9] seismic provisions. By employing these elastic acceleration response spectra, rock site peak ground acceleration (PGA) with 475 years' return period, importance factor of structure, and structural behavior factor design acceleration response spectra would be created. As regards the spectral matching results for obtaining appropriate synthetic earthquake acceleration time histories (EATHs) based on the obtained probabilistic uniform hazard spectra for the interested site, for each seismic hazard level, different EATHs can be obtained for dynamic structural analysis purposes. The derived EATHs are obtained through original filtered earthquake acceleration records due to the shallow crustal and subduction intraslab seismic sources of Malaysia.

3. Results

A seismic hazard curve is determined for a specific period of vibration at several motion stages, and the design value of acceleration for a specific period of vibration is obtained by interpolation of the hazard curve at 2%, 5%, or 10% probability of exceedance. The hazard curves for the mean annual rate of exceedance versus peak ground acceleration (PGA) for Sabah are compared with Sarawak and West Malaysia, as shown in Figure 5. This hazard curve is pertinent to the highest PGA in each region and is appropriate, for a rock site was derived from a source model that considers three segments of Sabah localized fault regions. Since the 2004 Aceh earthquake, Malaysian seismic hazard analysis has progressed steadily, beginning with the introduction of a rational framework for dealing with apparent randomness in earthquake processes, which allowed risk assessments to consider both the severity and likelihood of earthquake effects. The next stage was to identify epistemic uncertainties associated with inadequate knowledge and to develop frameworks for both quantifying and incorporating them into hazard evaluations. Structure shall be considered to have a return period, Tr of seismic action for the no-collapse requirement (or, equivalently, reference probability of exceedance in 50 years, when the following Equation (9) is satisfied

in unit of g (m/s^2) or gal (cm/s^2), where 1 g = 980 gal. Tr is the return period, q is the percent probability of exceedance (10%, 5%, or 2%), and t is the exposure time.

$$T_r = \frac{1}{1-(1-q)^{1/t}} \quad (9)$$

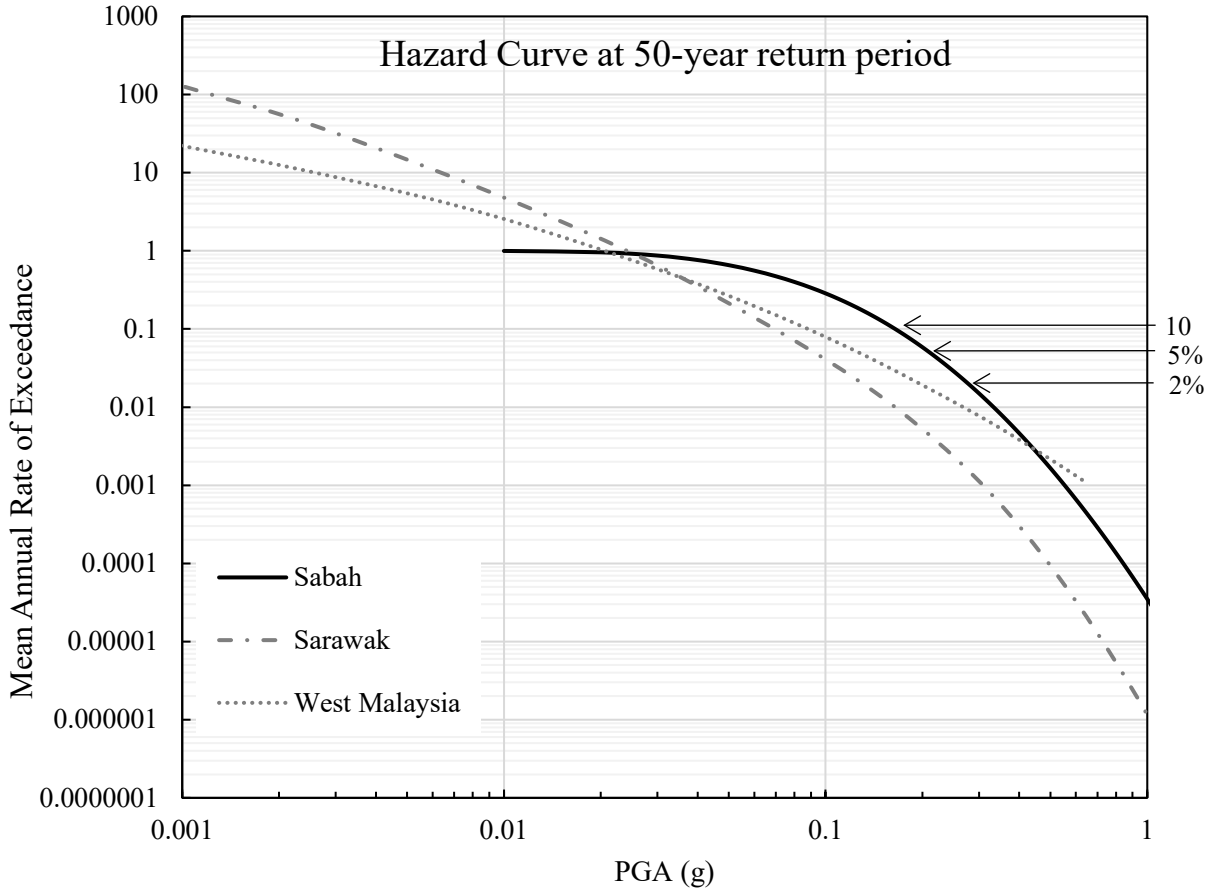

Figure 5. Sabah's hazard curves in comparison with the seismic zone of Sarawak and West Malaysia.

The hazard curve depicts peak ground acceleration with 10%, 5%, and 2% probabilities of exceeding in 50 years, corresponding to return periods of 475, 1000, and 2475 years, respectively. Sabah has the highest PGA rating [7], and earthquakes are common in the region. In the final analysis, from the hazard curve, it showed that the PGA value at 10% is equal to 0.16 g, 5% is 0.21 g, and 2% is 0.28 g by referring to the area of Sabah. In comparison with the hazard curve of Sarawak and West Malaysia developed by Ahmadi et al. [43] and Loi et al. [44] and summarized in Table 4, the study shows only 10% probability of exceedance, and the plot of hazard curve shows a different result of return period. From the analysis, 10% PE from Sarawak is equal to 0.07 g, 5% PE is 0.092 g, and 2% is equal to 0.13 g. As for West Malaysia, 10%, 5%, and 2% PE are equal to 0.09, 0.13, and 0.20 g, respectively. The PGA value of 10% PE in Sabah is equivalent to that suggested by MSEN1998-1:2015 [7]; however, different values found in Sarawak and West Malaysia predicted a lower value in comparison with MSEN1998-1:2015 [7]. MSEN1998-1:2015 [7] provides the hazard map for 10%, while Figures 6 and 7 provide the hazard maps for 5% and 2%, respectively. The term "uniform hazard spectrum" refers to a response spectrum where each point has the same probability of exceeding during a particular design time. In this work, the uniform hazard spectra (5% damping) of Ranau regions of Sabah were carried out to suggest design response spectral acceleration (RSA) on a bedrock for the entire Sabah region (Figure 8).

Table 4. Seismic hazard curve comparison values between Sabah, Sarawak, and West Malaysia at 10%, 5%, and 2% probability of exceedance.

Region	10%	5%	2%
Sabah	0.16 g	0.21 g	0.28 g
Sarawak	0.07 g	0.09 g	0.13 g
West Malaysia	0.09 g	0.13 g	0.20 g

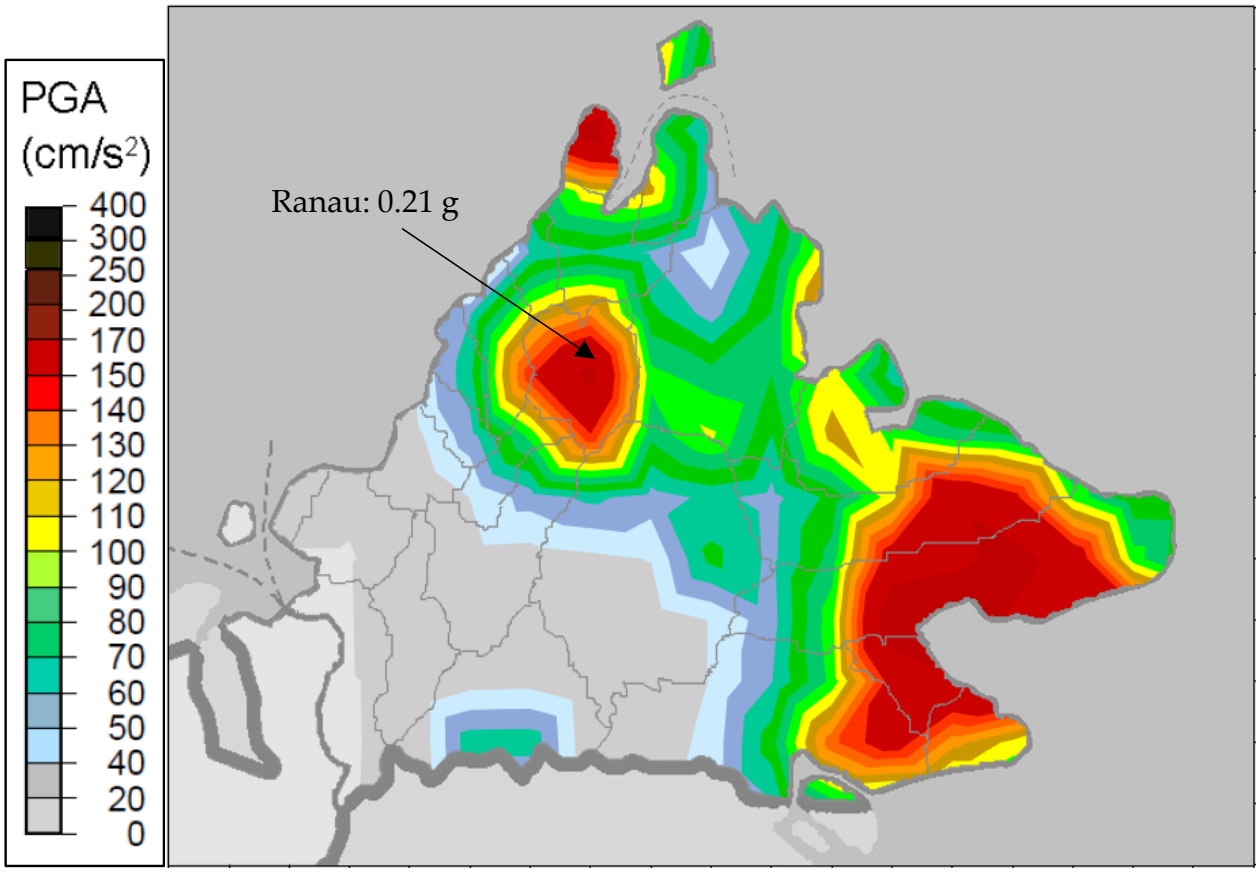

Figure 6. Sabah's hazard map at 5% probability of exceedance.

The seismic hazard study in Sabah is primarily determined by the seismicity of the region and the repercussions of previous failures. Many buildings were damaged as a result of the Ranau 6.0 magnitude earthquake, and the earthquake resulted in casualties and economic loss. Several studies, including Khoiry et al. [45], Roslee et al. [46], Ganasan et al. [47], and Razak et al. [48], discuss the analysis of structural integrity and construction measures, such as conceptual design, structural integrity, structural stiffness, strong column–weak beam, building construction, and seismic defect. All essential aspects affecting the seismic hazard at the specific site, as well as the actual dynamic performance of the structure, should be considered in structural analyses. As a result, the findings can be utilized to inform design or evaluation decisions, as well as the development of corrective procedures for Malaysian structures.

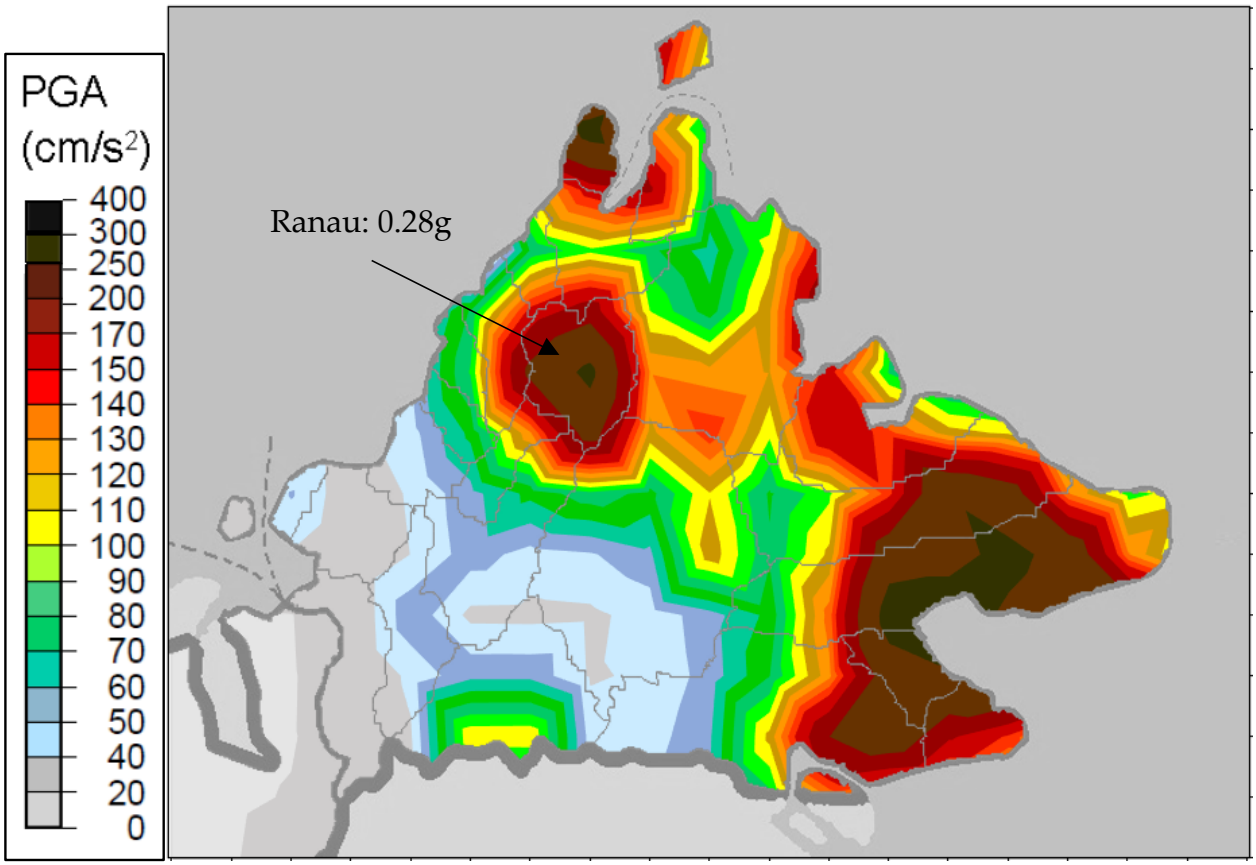

Figure 7. Sabah's hazard map at 2% probability of exceedance.

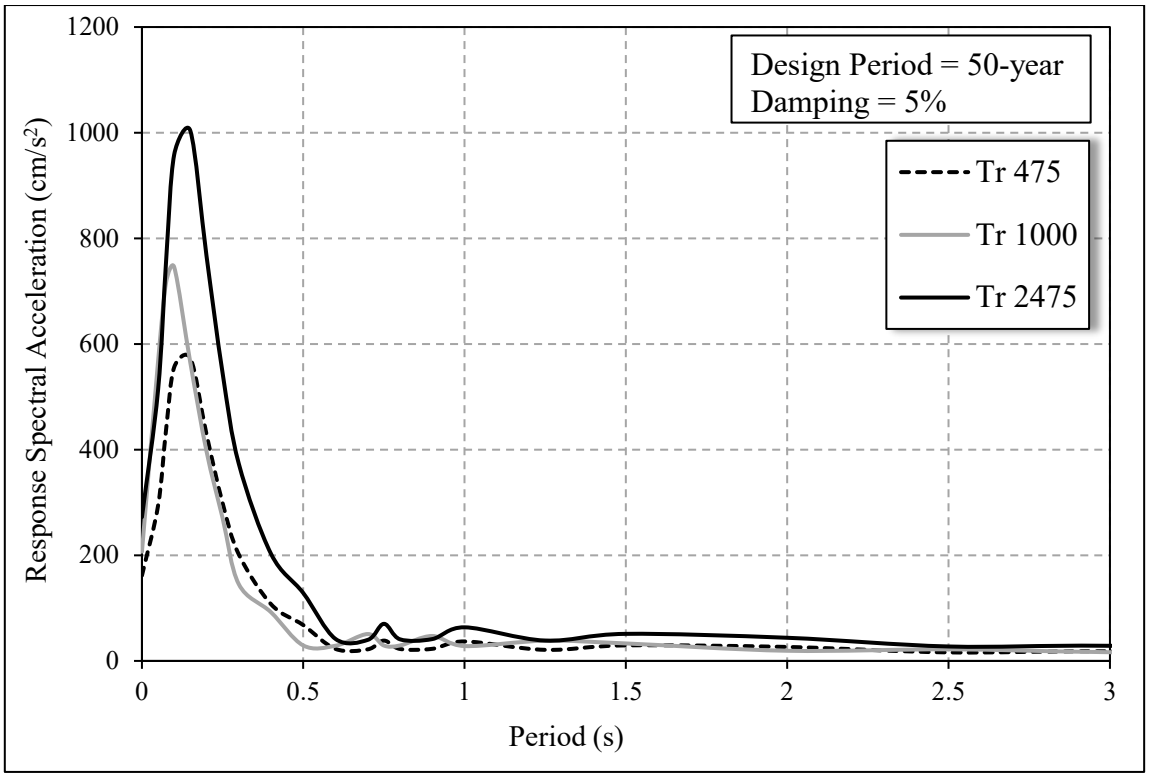

Figure 8. Uniform hazard spectra of Ranau regions in Sabah.

4. Conclusions

The probabilistic seismic hazard analysis (PSHA) is used in this study to estimate the hazard level of the Sabah region, which is applicable throughout Malaysia. This is because the region has the highest peak ground acceleration (PGA) of any state in Malaysia. The value can be used in building seismic design analysis. The hazard curve results were presented in this study using a combination of the region's local faults. Line, area, and background point source were used to model seismic sources with variable characteristics. From 1900 to 2021, the study region's composite earthquake catalogue includes a region bounded by 4 °S–8 °N latitude and 115 °E–120 °E longitude. In order to understand epistemic uncertainty, a logic tree structure was used to integrate simple quantities, such as maximum magnitudes and ground motion models (GMMs). The hazard curve for Malaysia was computed using probabilistic analysis at 10%, 5%, and 2% probability of exceedance (PE) in the design period of 50 years, which corresponds to return periods of approximately 475, 1000, and 2475 years, respectively. The PGA values at the bedrock were estimated to be about 0.16, 0.21, and 0.28 g for 10%, 5%, and 2% PE, respectively. The hazard curve value, however, can be applied when the value of PGA is similar; however, it does not apply for the region where the PGA values are lower than the suggested PGA.

The findings can be used to make design or evaluation decisions in Malaysia and to develop corrective procedures and anticipate structural failure in a variety of settings of 10%, 5%, or 2% PE. The application of a hazard curve in the current study might be applied in certain places around Malaysia if the PGA value is equivalent. For research purposes, some studies have used the highest PGA for damage prediction purposes in which the objective of this study is performed, where the current seismic design code are limited to the 10% seismic level. This study can be referenced to extend the rare event of the seismic level by applying two different seismic loads: 5% and 2%. The current seismic input can be extended to nonlinear dynamic analyses of structures in terms of acceleration time series whose response spectra are compatible with a specified target response spectrum. Generate synthetic ground motion appropriate for a site due to those return periods of earthquake. Carry out with the distribution percentage of hazard due to the considered seismic sources through disaggregation seismic hazard analysis.

Author Contributions: Conceptualization, N.S.H.H. and A.A.; methodology, N.S.H.H., F.T. and A.A.; software, N.S.H.H.; validation, F.T. and A.A.; formal analysis, N.S.H.H.; investigation, N.S.H.H., F.T. and A.A.; resources, N.S.H.H., F.T. and A.A.; data curation, N.S.H.H., F.T. and A.A.; writing—original draft preparation, N.S.H.H.; writing—review and editing, N.S.H.H.; visualization, N.S.H.H.; supervision, F.T. and A.A.; project administration, F.T. and A.A.; funding acquisition, N.S.H.H. All authors have read and agreed to the published version of the manuscript.

Funding: This research was funded by the Ministry of Higher Education Malaysia, grant number FRGS/1/2020/TK0/UMS/02/11.

Data Availability Statement: Data available on request due to restrictions eg privacy or ethical. The data presented in this study are available on request from the corresponding author. The data are not publicly available due to ethical concerns.

Conflicts of Interest: The authors declare no conflict of interest.

References

1. Alberto, P.; Igor, L.; Roberto, N. Seismic vulnerability assessment of an infilled reinforced concrete frame structure designed for gravity load. *J. Earthq. Eng.* **2017**, *21*, 267–289.
2. Perrone, D.; Calvi, P.M.; Nascimbene, R.; Fischer, E.C.; Magliulo, G. Seismic performance of non-structural elements during the 2016 Central Italy earthquake. *Bull. Earthq. Eng.* **2019**, *17*, 5655–5677. [CrossRef]
3. Hutchings, S.J.; Mooney, W.D. The seismicity of Indonesia and tectonic implications. *Geochem. Geophys. Geosystems* **2021**, *22*, 1–42. [CrossRef]
4. Muhd Yusrizal, Z.A.; Moosom, V.S.; Ismadi, P.N.N.; Farish, M.M.L.B.M.M.; Sulaiman, S.S.B. Is Malaysia Located in The Pacific Ring of Fire? A Legal Perspective. In *Law, Environment and Society*, 1st ed.; Kamaruddin, H., Tan, S., Thambusamy, R.X., Eds.; Future Academy, Universiti Kebangsaan Malaysia (UKM): Bangi, Malaysia, 2019; pp. 181–189.

5. Borah, N.; Kumar, A.; Dhanotiya, R. Seismic source zonation for NE India on the basis of past EQs and spatial distribution of seismicity parameters. *J. Seismol.* **2021**, *25*, 1483–1506. [CrossRef]
6. Sawires, R.; Peláez, J.A.; Hamdache, M. Probabilistic Seismic Hazard Assessment for United Arab Emirates, Qatar and Bahrain. Seismic source zonation for NE India on the basis of past EQs and spatial distribution of seismicity parameters. *Appl. Sci.* **2020**, *10*, 7901. [CrossRef]
7. *MSEN1998-1:2015*; Malaysia National Annex to Eurocode 8: Design of Structures for Earthquake Resistance—Part 1: General Rules, Seismic Actions and Rules for Buildings. 1st ed. Department of Standards Malaysia: Kuala Lumpur, Malaysia, 2017; pp. 1–39.
8. Drouet, S.; Ameri, G.; Le Dortz, K.; Secanell, R.; Senfaute, G. A probabilistic seismic hazard map for the metropolitan France. *Bull. Earthq. Eng.* **2020**, *18*, 1865–1898. [CrossRef]
9. *Eurocode 8*; Design of Structures for Earthquake Resistance—Part 1: General Rules, Seismic Actions and Rules for Buildings. 1st ed. European Committee for Standardization, The European Union: Brussels, Belgium, 2004; pp. 1–231.
10. Sharon, M.; Sagy, A.; Kurzon, I.; Marco, S.; Rosensaft, M. Assessment of seismic sources and capable faults through hierarchic tectonic criteria: Implications for seismic hazard in the Levant. *Nat. Hazards Earth Syst. Sci.* **2020**, *05*, 125–148. [CrossRef]
11. Wannier, M. History of geological mapping in Sabah (late 19th Century-1951). *Bull. Geol. Soc. Malays.* **2017**, *64*, 37–49. [CrossRef]
12. Mohd Zainudin, M.S.F.; Zubir, N.; Yan, A.S.W.; Amnan, I.; Among, H.L.; Javino, F. *Geological Map of Sabah*, 1st ed.; Minerals and Geoscience Malaysia: Kota Kinabalu, Malaysia, 2015; p. 1.
13. Agarwal, J.; Blockley, D. Structural integrity: Hazard, vulnerability and risk. *Int. J. Mater. Struct. Integr.* **2007**, *1*, 117–127. [CrossRef]
14. Looi, D.T.W.; Lam, N.; Tsang, H.H. Developing Earthquake-Resistant Structural Design Standard for Malaysia Based on Eurocode 8: Challenges and Recommendations. *Standards* **2021**, *1*, 134–153. [CrossRef]
15. Chong, J.H.; Alih, S.C.; Vafaei, M.; Wong, W.K. Seismic Performance of Low Ductile RC Frame Designed in Accordance with Malaysia National Annex to Eurocode 8. *IOP Conf. Ser. Earth Environ. Sci.* **2021**, *682*, 012011. [CrossRef]
16. Looi, D.T.W.; Tsang, H.H.; Hee, M.C. Seismic Hazard Modelling for Malaysia and Singapore. In Proceedings of the 2017 World Congress on Advances in Structural Engineering and Mechanics (ASEM17), Ilsan, Seoul, Republic of Korea, 28 August–1 September 2017.
17. Pagani, M.; Garcia-Pelaez, J.; Gee, R.; Johnson, K.; Poggi, V.; Silva, V.; Simionato, M.; Styron, R.; Vigano, D.; Danciu 10, L. The 2018 version of the Global Earthquake Model: Hazard component. *Earthq. Spectra* **2020**, *36*, 226–251. [CrossRef]
18. Yang, Y.; Shi, B.; Sun, L. Seismic hazard estimation based on the distributed seismicity in northern China. *Earthq. Sci.* **2008**, *21*, 202–212. [CrossRef]
19. Dutfoy, A. Estimation of the Gutenberg–Richter earthquake recurrence parameters for unequal observation periods and imprecise magnitudes. *Pure Appl. Geophys.* **2020**, *177*, 4597–4606. [CrossRef]
20. Al Atik, L.; Abrahamson, N. An improved method for nonstationary spectral matching. *Earthq. Spectra* **2010**, *26*, 601–617. [CrossRef]
21. Marmureanu, G.; Cioflan, C.O.; Marmureanu, A.; Ionescu, C.; Manea, E.F. Bridging the Gap Between Nonlinear Seismology as Reality and Earthquake Engineering. In *Perspectives on European Earthquake Engineering and Seismology*, 1st ed.; Ansal, A., Ed.; Geotechnical, Geological and Earthquake Engineering: Istanbul, Turkey, 2015; Volume 2, pp. 409–428.
22. Solarino, F.; Giresini, L. Fragility curves and seismic demand hazard analysis of rocking walls restrained with elasto-plastic ties. *Earthq. Eng. Struct. Dyn.* **2021**, *50*, 3602–3622. [CrossRef]
23. Vargas-Alzate, Y.F.; Hurtado, J.E.; Pujades, L.G. New insights into the relationship between seismic intensity measures and nonlinear structural response. *Bull. Earthq. Eng.* **2022**, *20*, 2329–2365. [CrossRef]
24. Jorge, L.A.; José, A.R.; Rossana, V. Unification of different approaches to probabilistic seismic hazard analysis. *Bull. Seismol. Soc. Am.* **2020**, *110*, 2816–2827.
25. Beauval, C.; Bard, P.Y. History of probabilistic seismic hazard assessment studies and seismic zonations in mainland France. *Géoscience* **2021**, *353*, 413–440. [CrossRef]
26. Lamessa, G.; Mammo, T.; Raghuvanshi, T.K. Homogenized earthquake catalog and b-value mapping for Ethiopia and its adjoining regions. *Geoenviron. Disasters* **2019**, *6*, 1–24. [CrossRef]
27. Ghasemi, H.; Cummins, P.; Weatherill, G.; McKee, C.; Hazelwood, M.; Allen, T. Seismotectonic model and probabilistic seismic hazard assessment for Papua New Guinea. *Bull. Earthq. Eng.* **2020**, *18*, 6571–6605. [CrossRef]
28. Sianko, I.; Ozdemir, Z.; Khoshkholghi, S.; Garcia, R.; Hajirasouliha, I.; Yazgan, U.; Pilakoutas, K. A practical probabilistic earthquake hazard analysis tool: Case study Marmara region. *Bull. Earthq. Eng.* **2020**, *18*, 2523–2555. [CrossRef]
29. Ranjit, D.; Claudio, M. A unified moment magnitude earthquake catalog for Northeast India. *Geomat. Nat. Hazards Risk* **2021**, *12*, 167–180.
30. Leptokaropoulos, K.M.; Gkarlaouni, C.G. A magnitude independent space-time earthquake clustering algorithm. *Bull. Geol. Soc. Greece* **2016**, *50*, 1359–1368. [CrossRef]
31. Zaliapin, I.; Ben-Zion, Y. Earthquake declustering using the nearest-neighbor approach in space-time-magnitude domain. *J. Geophys. Res.* **2020**, *125*, 1–33. [CrossRef]
32. Cesca, S.S. A tool for density-based seismicity clustering and visualization. *J. Seismol.* **2020**, *24*, 443–457. [CrossRef]

33. Pagani, M.; Monelli, D.; Weatherill, G.; Danciu, L.; Crowley, H.; Silva, V.; Henshaw, P.; Butler, R.; Nastasi, M.; Panzeri, L.; et al. OpenQuake engine: An open hazard (and risk) software for the Global Earthquake Model. *Seismol. Res. Lett.* **2014**, *85*, 692–702. [CrossRef]
34. Anbazhagan, P.; Bajaj, K.; Matharu, K.; Moustafa, S.S.R.; Al-Arifi, N.S.N. Probabilistic seismic hazard analysis using the logic tree approach—Patna district (India). *Nat. Hazards Earth Syst. Sci.* **2019**, *19*, 2097–2115. [CrossRef]
35. Weatherill, G.; Cotton, F. A ground motion logic tree for seismic hazard analysis in the stable cratonic region of Europe: Regionalisation, model selection and development of a scaled backbone approach. *Bull. Earthq. Eng.* **2020**, *18*, 6119–6148. [CrossRef]
36. Abrahamson, N.; Silva, W. Summary of the Abrahamson & Silva NGA ground-motion relations. *Earthq. Spectra* **2008**, *24*, 67–97.
37. Zhao, J.X.; Zhang, J.; Asano, A.; Ohno, Y.; Oouchi, T.; Takahashi, T.; Ogawa, H.; Irikura, K.; Thio, H.K.; Somerville, P.G.; et al. Attenuation relations of strong ground motion in Japan using site classification based on predominant period. *Bull. Seismol. Soc. Am.* **2006**, *96*, 898–913. [CrossRef]
38. Fukushima, Y.; Tanaka, T. The revision of A New Attenuation Relation for Peak Horizontal Acceleration of Strong Earthquake Ground Motion in Japan. *Abstr. Seismol. Soc. Jpn.* **1992**, *1*, B18.
39. Van, T.C.; Lau, T.L.; Mok, C.F. Selection of ground motion attenuation model for Peninsular Malaysia due to far-field Sumatra earthquakes. *Nat. Hazards* **2015**, *80*, 1865–1889. [CrossRef]
40. Cummins, P.R. Geohazards in Indonesia: Earth science for disaster risk reduction-introduction. *Geol. Soc.* **2017**, *441*, 1–7. [CrossRef]
41. Taroni, M.; Selva, J.; Zhuang, J. Estimation of the tapered Gutenberg-Richter distribution parameters for catalogs with variable completeness: An application to the Atlantic ridge seismicity. *Appl. Sci.* **2021**, *11*, 12166. [CrossRef]
42. Baker, J.W.; Bradley, B.A.; Stafford, P.J. *Seismic Hazard and Risk Analysis*, 1st ed.; Cambridge University Press: Cambridge, UK, 2021; pp. 1–600.
43. Ahmadi, R.; Ahmad, A.; Abdullahi, A.F.; Najar, I.A.; Muhamad Suhaili, M.H.A. A Framework on Site-Specific Probabilistic Seismic Hazard Assessment of Tabung Haji Hotel and Convention Centre in Kuching, Sarawak, Malaysia. Available online: https://www.researchgate.net/publication/336207830_A_framework_on_site-specific_probabilistic_seismic_hazard_assessment_of_Tabung_Haji_hotel_and_Convention_centre_in_Kuching_Sarawak_Malaysia (accessed on 1 November 2022).
44. Loi, D.; Raghunandan, M.; Swamy, V. Revisiting seismic hazard assessment for Peninsular Malaysia using deterministic and probabilistic approaches. *Nat. Hazards Earth Syst. Sci.* **2018**, *18*, 2387–2408. [CrossRef]
45. Khoiry, M.A.; Hamzah, N.; Osman, S.; Mutalib, A.; Hamid, R. Physical damages effect on residential houses caused by the earthquake at Ranau, Sabah Malaysia. *Int. J. Eng. Technol.* **2018**, *10*, 414–418. [CrossRef]
46. Roslee, R.; Termizi, A.K.; Indan, E.; Tongkul, F. Earthquake vulnerability assessment (EVAs): Analysis of environmental vulnerability and social vulnerability in Ranau area, Sabah, Malaysia. *Geol. Behav.* **2018**, *2*, 24–28.
47. Ganasan, R.; Tan, C.G.; Ibrahim, Z.; Mohamed Nazri, F.; Wong, H. A Case Study on Structural Failure of Reinforced Concrete Beam-Column Joint After the First Significant Earthquake Impact in Malaysia. *Int. J. Integr. Eng.* **2020**, *12*, 288–302. [CrossRef]
48. Razak, J.; Rambat, S.; Che Ros, F.; Shi, Z.; Mazlan, S. Seismic vulnerability assessment in Ranau, Sabah, using two different models. *Int. J. Geo-Inf.* **2021**, *10*, 1–25.